J. Am. Chem. Soc. **1992,** *114,* 5125–5130

Low-Temperature Neutron Diffraction Study of $HMn_2Re(CO)_{14}$ and Studies of a Metal–Metal Exchange Equilibrium That Converts $HMn_2Re(CO)_{14}$ into $HMnRe_2(CO)_{14}$

R. Morris Bullock,*,[1a] Lee Brammer,[1a,d] Arthur J. Schultz,[1b] Alberto Albinati,[1c] and Thomas F. Koetzle*,[1a]

Contribution from the Department of Chemistry, Brookhaven National Laboratory, Upton, New York 11973, the Chemistry and Materials Science Divisions, Argonne National Laboratory, Argonne, Illinois 60439, and the Institute of Pharmaceutical Chemistry, University of Milan, I-20131 Milan, Italy. *Received August 29, 1991*

Abstract: The crystal and molecular structure of $(CO)_5Re(\mu\text{-}H)Mn(CO)_4Mn(CO)_5$, prepared from reaction of $Mn_2(CO)_9(\eta^1\text{-tolualdehyde})$ with $HRe(CO)_5$, has been determined from neutron diffraction measurements at 15 K: unit-cell constants, $a = 9.145$ (1) Å, $b = 15.557$ (3) Å, $c = 14.040$ (3) Å, $\beta = 106.60$ (2)°, monoclinic, space group $P2_1/n$, $Z = 4$, $V = 1914.2$ (6) Å^3. $R(F^2) = 0.110$ for 4859 reflections with $F_0^2 \geq 3\sigma(F_0^2)$ and $(\sin\theta/\lambda)_{max} = 1.054$ Å^{-1}. The Re–H distance (1.827 (4) Å) is longer than the Mn–H distance (1.719 (5) Å). Spectroscopic and crystallographic data indicate that a small amount (~9%) of $(CO)_5Re(\mu\text{-}H)Mn(CO)_4Re(CO)_5$ has cocrystallized with the major component. Further evidence for the identity of $(CO)_5Re(\mu\text{-}H)Mn(CO)_4Re(CO)_5$ comes from an independent synthesis by a known route. A mechanism is proposed that accounts for the formation of $(CO)_5Re(\mu\text{-}H)Mn(CO)_4Re(CO)_5$ from the reaction of $(CO)_5Re(\mu\text{-}H)Mn(CO)_4Mn(CO)_5$ with $HRe(CO)_5$. The equilibrium constant for the metal–metal exchange equilibrium, $(CO)_5Re(\mu\text{-}H)Mn(CO)_4Mn(CO)_5 + HRe(CO)_5 \rightleftharpoons (CO)_5Re(\mu\text{-}H)Mn(CO)_4Re(CO)_5 + HMn(CO)_5$, has been determined; $K_{eq} = 1.00 \pm 0.05$ at 22 °C in C_6D_6.

Introduction

Heterometallic complexes have been studied extensively,[2] partly due to their potential utility in catalytic reactions. The importance of metal hydrides in numerous catalytic reactions suggests that precise structural information on hydrides bridging between two different metals[3] will be useful in the further development and understanding of these complexes. We have recently reported[4] an X-ray diffraction study of $(CO)_5Re(\mu\text{-}H)Mn(CO)_4Mn(CO)_5$ (**1**), which was prepared from the reaction of $Mn_2(CO)_9(\eta^1\text{-tolualdehyde})$ with excess $HRe(CO)_5$ as shown in eq 1. NMR spectroscopic data indicated the presence in the sample of a small amount of an impurity, with an upfield ^{1}H NMR chemical shift consistent with a bridging hydride. In this paper we report a single-crystal neutron diffraction study of **1**, which provides an accurate determination of the geometry of the $Re(\mu\text{-}H)Mn$ bridge. Along with the diffraction measurements, spectroscopic data and independent synthesis demonstrate that the impurity that cocrystallized with the major product is $(CO)_5Re(\mu\text{-}H)Mn(CO)_4Re(CO)_5$ (**2**). An equilibrium constant is reported for an unusual metal–metal exchange reaction that interchanges Mn and Re between mononuclear $HM(CO)_5$ species and the terminal $M(CO)_5$ units on the trimetallic cluster.

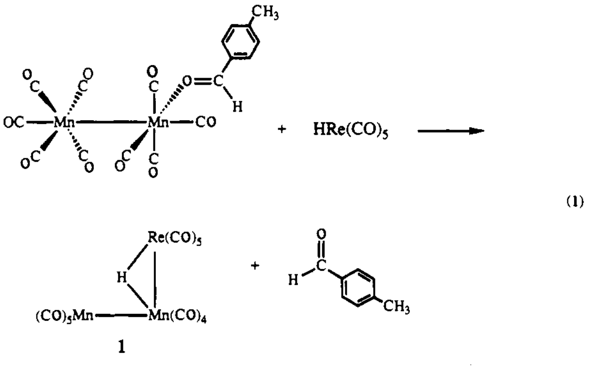

(1)

1

Experimental Section

General. All manipulations were carried out under an atmosphere of nitrogen or argon using Schlenk or vacuum-line techniques or in a Vacuum Atmospheres drybox. NMR spectra were recorded on a Bruker AM-300 spectrometer (300 MHz for ^{1}H). IR spectra were recorded on a Mattson Polaris FT-IR spectrometer, using CaF_2 cells. C_6D_6 was dried over NaK, stored over $(Cp_2TiCl)_2ZnCl_2$,[5] and vacuum transferred into the NMR tubes. $HMn(CO)_5$ and $HRe(CO)_5$ were prepared by a published procedure[6] and dried over P_2O_5. These hydrides were stored under vacuum at −20 °C in the dark and vacuum transferred immediately prior to each use. $CH_3Mn(CO)_5$ was prepared by M. A. Andrews for an earlier study.[7]

$(CO)_5Re(\mu\text{-}H)Mn(CO)_4Mn(CO)_5$ (1) was prepared from $Mn_2(CO)_9(\eta^1\text{-tolualdehyde})$ and $HRe(CO)_5$ as described previously.[4] The ^{1}H NMR spectrum (C_6D_6) exhibits a peak for **1** at δ −19.66 (s); a singlet at δ −19.24 (~10% of the intensity of the major peak) was also observed and is due to $(CO)_5Re(\mu\text{-}H)Mn(CO)_4Re(CO)_5$ (**2**). IR (hexane): 2147 w, 2086 w, 2047 s, 2014 m, 1989 m, 1984 m, 1974 m, 1961 w, 1933 w cm^{-1}. A solution of **1** in CH_2Cl_2 in a Schlenk tube was layered with hexane. Slow mixing of the solvents at −20 °C produced large red-orange crystals suitable for neutron diffraction. The crystals were washed with hexane and dried briefly under vacuum.

$(CO)_5Re(\mu\text{-}H)Mn(CO)_4Re(CO)_5$ (2) was prepared by a minor modification of the published procedure.[6] A solution of $CH_3Mn(CO)_5$ (77 mg, 0.37 mmol) and $HRe(CO)_5$ (267 mg, 0.81 mmol, 2.2 equiv) in toluene (2 mL) was left at room temperature in the dark (without stirring) for 4.5 days. The orange-yellow crystalline product was washed with hexane and dried under vacuum to give **2** (211 mg, 0.26 mmol, 70% yield). ^{1}H NMR (C_6D_6): δ −19.24 (s). IR (hexane): 2145 w, 2104 w,

---

(1) (a) Brookhaven National Laboratory. (b) Argonne National Laboratory. (c) University of Milan. (d) Present address: Department of Chemistry, University of Missouri—St. Louis, St. Louis, MO 63121.

(2) For reviews of heterometallic complexes, see: (a) Roberts, D. A.; Geoffroy, G. L. In *Comprehensive Organometallic Chemistry*; Wilkinson, G., Stone, F. G. A., Abel, E. W., Eds.; Pergamon: Oxford, 1982; Vol. 6, Chapter 40. (b) Stephan, D. W. *Coord. Chem. Rev.* **1989,** *95,* 41–107. (c) Bullock, R. M.; Casey, C. P. *Acc. Chem. Res.* **1987,** *20,* 167–173.

(3) For a review of metal complexes with bridging hydrides, see: Venanzi, L. M. *Coord. Chem. Rev.* **1982,** *43,* 251–274. See also: Teller, R. G.; Bau, R. *Struc. Bonding* **1981,** *44,* 1–82; Gomes Carneiro, T. M.; Matt, D.; Braunstein, P. *Coord. Chem. Rev.* **1989,** *96,* 49–88; Mueting, A. M.; Bos, W.; Alexander, B. D.; Boyle, P. D.; Casalnuovo, J. A.; Balaban, S.; Ito, L. N.; Johnson, S. M.; Pignolet, L. H. *New J. Chem.* **1988,** *12,* 505–527.

(4) Albinati, A.; Bullock, R. M.; Rappoli, B. J.; Koetzle, T. F. *Inorg. Chem.* **1991,** *30,* 1414–1417.

(5) Sekutowski, D. G.; Stucky, G. D. *Inorg. Chem.* **1975,** *9,* 2192–2199.

(6) Warner, K. E.; Norton, J. R. *Organometallics* **1985,** *4,* 2150–2160.

(7) Andrews, M. A.; Eckert, J.; Goldstone, J. A.; Passell, L.; Swanson, B. *J. Am. Chem. Soc.* **1983,** *105,* 2262–2269.

0002-7863/92/1514-5125$03.00/0

2044 s, 2028 w, 2016 w, sh, 2011 m, 1998 m, 1976 m, 1953 w, 1944 w, 1927 w cm^{-1}.

Reactions of CO with 1 and 2. A yellow-orange solution of **2** (~0.01 M in C_6D_6) containing 1,4-bis(trimethylsilyl)benzene as an internal standard was prepared, and an initial ^1H NMR spectrum was recorded. CO (1 atm) was added, and the solution was shaken several times over the next few minutes. An NMR spectrum taken at $t \approx 5$ min showed that the reaction was partially complete. The color of the solution faded to pale yellow during the reaction. An NMR spectrum taken at $t \approx 30$ min indicated that all of the **2** had reacted, and a quantitative yield of $HRe(CO)_5$ (δ −5.62) was observed. The volatiles (i.e., $HRe(CO)_5$ and C_6D_6) were evaporated, and the residue was redissolved in hexane. An IR spectrum showed bands due to $MnRe(CO)_{10}$ (2125 w, 2055 m, 2033 vw, 2018 s, 1999 w, 1993 vw, 1979 m, 1946 vw cm^{-1}, in excellent agreement with the literature values[8]) and no bands due to $Mn_2(CO)_{10}$. In a similar experiment, a light orange solution of **1** in C_6D_6 was treated with CO (1 atm), and the solution turned yellow within a few minutes. The singlet for **1** at δ −19.66 was replaced by a singlet for $HRe(CO)_5$ (δ −5.62). The volatiles were removed by evaporation, and the residue was dissolved in hexane. The IR spectrum showed $Mn_2(CO)_{10}$[8] (2046 m, 2014 s, 2003 w, 1984 m cm^{-1}) as the predominant product. Weaker bands in the IR spectrum were observed for $MnRe(CO)_{10}$, which forms from the **2** impurity in **1**.

Determination of K_{eq} for the Metal–Metal Exchange Equilibrium. The equilibrium constant K_{eq} for $(CO)_5Re(\mu\text{-}H)Mn(CO)_4Mn(CO)_5$ + $HRe(CO)_5 \rightleftharpoons (CO)_5Re(\mu\text{-}H)Mn(CO)_4Re(CO)_5 + HMn(CO)_5$ (eq 4, vide infra) was determined by ^1H NMR measurements in C_6D_6 solutions at 22 °C. A delay of 30 s between pulses was used to ensure accurate integrations; use of a 60-s delay did not give appreciably different integrations. A solution of either **1** or **2** (initial concentration 0.014–0.02 M) was treated with an excess of both $HRe(CO)_5$ and $HMn(CO)_5$ (initial concentration 0.1–0.9 M in each mononuclear hydride). The equilibrium was established within ~1 h. Equilibrium constants were determined for two tubes starting with **2** and for one tube starting with **1**. The measured K_{eq} values were indistinguishable within experimental error for the three experiments. The average value (and standard deviation) from nine separate measurements on the three different solutions gave K_{eq} = 1.00 ± 0.05.

Neutron Diffraction Study. Neutron intensity measurements were made by using the Laue time-of-flight method on the single crystal diffractometer (SCD) at the Argonne Intense Pulsed Neutron Source (IPNS). The instrumentation and the procedure for data collection and data reduction for the IPNS-SCD have been detailed in previous articles[9-11] and will be described here in more general terms, with detail given only of differences from the previously reported procedures.

The two primary differences from the experimental setup and procedures described in ref 9 are, first, that the pulsed spallation process used to generate neutrons now uses an *enriched* uranium target and, second, that data were collected at reduced temperature, the sample temperature being maintained at 15 ± 1 K during the course of the experiment using a Displex refrigerator.[12] Twenty-six crystal orientations were used in obtaining a unique quadrant of data, with measurement time at each setting being determined by a preset monitor count. Intensity data were recorded in histogram form, each neutron arrival at the detector being characterized by three digitized coordinates representing the position on the 30 × 30 cm^2 area detector (x and y) and the time-of-flight (t). Strong Bragg reflections located in each histogram were used in an autoindexing routine to obtain histogram-specific orientation matrices. The location of other reflections in a particular histogram was then predicted from its orientation matrix, and three-dimensional (x-y-t) intensity integrations were performed by using a fixed envelope size for all reflections. The envelope size was determined by trial integrations of the stronger reflections. As a result of the Bragg diffraction angles attainable with the SCD and the use of a range of neutron wavelengths, in measuring a unique sector of reciprocal space to a given resolution a limited sampling of reciprocal space to higher resolution is also obtained (see Table I).

Table I. Experimental Data for the Neutron Diffraction Study of $(CO)_5Re(\mu\text{-}H)Mn(CO)_4Mn(CO)_5$

formula	$C_{14}HO_{14}Mn_2Re$
mol wt	689.23
cryst dimens, mm	1.70 (diameter)
temp, K	15 (1)
cryst system	monoclinic
space group	$P2_1/n$
a, Å	9.145 (1)[a]
b, Å	15.557 (3)[a]
c, Å	14.040 (3)[a]
β, deg	106.60 (2)[a]
Z	4
V, Å^3	1914.2 (6)
ρ(calcd), g cm^{-3}	2.422 (1)
λ, Å	0.7–4.2
μ_n, cm^{-1}	0.472–3.209
calcd transmission factors	0.9098–0.9794
measd reflectns	full quadrant for $\sin\theta/\lambda <$ 0.767 Å^{-1}; partial quadrant $0.767 \le \sin\theta/\lambda < 1.205$ Å^{-1}
no. of data collected	21 923
no. of data used in refinement (n) [$F_o^2 \ge 3\sigma(F_o^2)$; λ = 0.8–4.0 Å; $(\sin\theta/\lambda)_{max}$ = 1.054 Å^{-1}; $F_c^2 > \lvert F_o^2 - F_c^2\rvert$; ext[b] ≥ 0.7]	4859
no. of variables refined (m)	317
functn minimized	$\sum w(F_o^2 - F_c^2)^2$
weights, w	$[\sigma^2 F_o^2 + (0.04F_o^2)^2]^{-1}$
$R(F^2)$[c]	0.110
$R_w(F^2)$[d]	0.101
$R(F)$[e]	0.062
$S(F^2)$[f]	1.095
extinction parameter, g	3.6 (1) × 10^3
neutron scattering lengths, fm	b_{Re} 9.54 (6) refined, b_{Mn} −3.73, b_O 5.803, b_C 6.646, b_H −3.7409

[a] Based on $\sin^2\theta$ values obtained from the centroids of 1310 reflections. [b] Extinction factor multiplying F_c^2. [c] $R(F^2) = \sum\lvert F_o^2 - F_c^2\rvert/\sum F_o^2$. [d] $R_w(F^2) = [\sum w(F_o^2 - F_c^2)^2/\sum wF_o^4]^{1/2}$. [e] $R(F) = \sum\lvert F_o - \lvert F_c\rvert\rvert/\sum F_o$. [f] $S(F^2) = [(\sum w(F_o^2 - F_c^2)^2)/(n - m)]^{1/2}$.

The data were corrected for wavelength-dependent incident flux and detector efficiency, using for calibration the incoherent scattering spectrum of a vanadium sample. A wavelength-dependent spherical absorption correction was applied.[13] The crystal, although slightly irregular in shape, was fairly equidimensional and thus was approximated by a sphere. The linear absorption coefficients were calculated for the minimum and maximum wavelengths used (0.7 and 4.2 Å), and a linear interpolation was used for values between these limits. Symmetry-related reflections were not averaged; being measured at different wavelengths, different extinction factors were applicable to each reflection.

Least-squares refinement of positional and anisotropic displacement parameters was undertaken, using as initial values those obtained from the room-temperature X-ray diffraction study.[4] Together with these parameters, independent scale factors for data measured in each crystal orientation and a parameter for wavelength-dependent isotropic extinction (Becker & Coppens formalism,[14] Type I, Lorentzian distribution) were included as variables. Final refinements were based on data associated with the incident wavelength range 0.8–4.0 Å, as inclusion of data from the full incident neutron wavelength range (0.7–4.2 Å) led to nonpositive definite displacement parameters for the metal atoms (see below). Experimental details are given in Table I.

Least-Squares Refinements. The structure was refined by full-matrix least squares, minimizing $\sum w(F_o^2 - F_c^2)^2$. Initially, with isotropic displacement parameters for the metal atoms, physically unreasonable U_{iso} values were obtained for both the Re and Mn(2) sites. For the former, a slightly negative value was obtained, while for the latter, mean-sequare amplitudes were approximately 7 times larger than those for Mn(1). Having established that systematic errors, particularly instrumental corrections, were not the primary source of these unusual values, the scattering lengths for the two sites were refined concurrently with previously noted parameters. With refinement of these scattering lengths, refinement of anisotropic displacement parameters for the metal sites also became feasible. The refinement behaved well, with all correlations between parameters remaining below 0.58 in absolute value. At con-

---

[8] Flitcroft, N.; Huggins, D. K.; Kaesz, H. D. *Inorg. Chem.* **1964**, *3*, 1123–1130.

[9] Schultz, A. J.; Srinivasan, K.; Teller, R. G; Williams, J. M.; Lukehart, C. M. *J. Am. Chem. Soc.* **1984**, *106*, 999–1003.

[10] Schultz, A. J. *Trans. Am. Crystallogr. Assoc.* **1987**, *23*, 61–69.

[11] Schultz, A. J.; Van Derveer, D. G.; Parker, D. W.; Baldwin, J. E. *Acta Crystallogr., Sect. C* **1990**, *46*, 276–279.

[12] Air Products and Chemicals, Inc.

[13] (a) Sears, V. F. In *Methods of Experimental Physics*; Skold, K., Price, D. L., Eds.; Academic Press: Orlando, FL, 1986; Vol. 23, Neutron Scattering, Part A, pp 521–550. (b) Howard, J. A. K.; Johnson, O.; Schultz, A. J.; Stringer, A. M. *J. Appl. Crystallogr.* **1987**, *20*, 120–122.

[14] Becker, P. J.; Coppens, P. *Acta Crystallogr., Sect. A* **1975**, *A31*, 417–425.

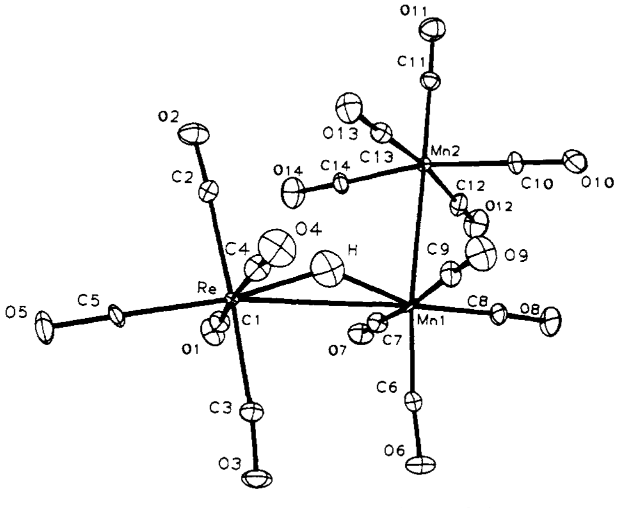

Figure 1. View of the $(CO)_5Re(\mu\text{-}H)Mn(CO)_4Mn(CO)_5$ molecule showing atom nomenclature, with ellipsoids drawn at the 90% probability level.

vergence, following further cycles of least squares, the values $b_{Re} = 9.54$ (6) fm and $b_{Mn(2)} = -2.67$ (5) fm (cf., literature values[13a] $b_{Re} = 9.20$ fm and $b_{Mn} = -3.73$ fm) were obtained. Two possible factors may be jointly responsible for this: (1) The reported value for b_{Re} of 9.20 fm is an underestimate. We have tested this hypothesis by refining the Re scattering length for the structure $[ReH_7\{P(p\text{-tolyl})_3\}_2]$,[15] for which data were measured at the Brookhaven National Laboratory High Flux Beam Reactor. A value of 9.55 (6) fm was obtained, i.e., consistent with that found here. (2) The refined value of $b_{Mn(2)}$ suggests partial occupancy of this site by rhenium (9.2%); i.e., the presence of the isomorphous product (**2**) cocrystallized with **1**. Re-examination of the displacement parameters obtained from the X-ray diffraction study[4] supported this assertion, Mn(2) having a value approximately 40% smaller than that for Mn(1).

A further refinement based on the previously collected X-ray data was carried out, assuming mixed occupancy for the Mn(2) site (occupancy factors of 0.9 and 0.1 were assigned for Mn and Re, respectively). After convergence, while the bond distances and angles did not change significantly, the displacement parameters of the Mn atoms were now comparable (U_{iso} 0.035 (1) and 0.038 (1) Å^2 for Mn(1) and Mn(2), respectively), the residual, $R(F)$, dropped from 0.031 to 0.024, and the goodness-of-fit (defined as $S(F) = [\Sigma w(F_0 - |F_c|)^2/(n_o - n_v)]^{1/2}$) was reduced from 1.321 to 0.912.

As noted above, the final neutron refinements were based upon data obtained within the incident wavelength range $0.8 < \lambda < 4.0$ Å rather than the full range (0.7–4.2 Å) for which intensities were measured. Refinements using the full wavelength range yielded nonpositive definite displacement parameters for Mn(1) and Mn(2), due to large off-diagonal terms in their U_{ij} tensors. Trial refinements were conducted for different wavelength ranges. These resulted in significant changes in the U_{ij}'s of the metal atoms but *no* significant changes in the values of other parameters. Hence, a wavelength range was selected so as to maximize the number of data used in refinement, while maintaining positive definite displacement parameters for all atoms. It is anticipated that the displacement parameters of the metal atoms, particularly Mn(1) and Mn(2), represent a composite of thermal motion and other effects. Such effects may include a small positional mismatch of metal atoms sites from the two cocrystallized compounds, together with any residual systematic errors. In order to investigate the former effect, rms amplitudes of vibration for the carbon and oxygen atoms parallel and perpendicular to the M–C–O axes were calculated. However, no systematic differences in magnitude were noted for carbonyl groups attached at different sites, indicating that the effect of positional mismatch is small. All calculations were carried out on MicroVAX computers using locally written (Argonne and Brookhaven) programs. Atomic positional and anisotropic displacement parameters are provided in the Supplementary Material (Table S1), together with a listing of observed and calculated squared structure factors (Table S2).

Results and Discussion

Structure. An ORTEP view of $(CO)_5Re(\mu\text{-}H)Mn(CO)_4Mn(CO)_5$ (**1**) is shown in Figure 1, while a list of relevant bond distances and angles is given in Table II.

Table II. Interatomic Distances (Å) and Angles (deg)

Re–Mn(1)	3.316 (3)	Mn(1)–Mn(2)	2.909 (6)
Re–H	1.827 (4)	Mn(1)–H	1.719 (5)
Re···Mn(2)	4.716 (4)		
Re–C(1)	1.997 (2)	Re–C(2)	2.021 (3)
Re–C(3)	2.016 (3)	Re–C(4)	2.032 (2)
Re–C(5)	1.948 (2)	Mn(1)–C(6)	1.808 (4)
Mn(1)–C(7)	1.860 (3)	Mn(1)–C(8)	1.815 (3)
Mn(1)–C(9)	1.860 (3)	Mn(2)–C(10)	1.880 (4)
Mn(2)–C(11)	1.809 (5)	Mn(2)–C(12)	1.870 (4)
Mn(2)–C(13)	1.848 (4)	Mn(2)–C(14)	1.855 (4)
C(1)–O(1)	1.139 (2)	C(2)–O(2)	1.130 (3)
C(3)–O(3)	1.134 (3)	C(4)–O(4)	1.131 (2)
C(5)–O(5)	1.146 (2)	C(6)–O(6)	1.152 (3)
C(7)–O(7)	1.140 (2)	C(8)–O(8)	1.145 (3)
C(9)–O(9)	1.144 (2)	C(10)–O(10)	1.137 (2)
C(11)–O(11)	1.151 (3)	C(12)–O(12)	1.141 (2)
C(13)–O(13)	1.148 (2)	C(14)–O(14)	1.138 (3)
C–O_{mean}[a]	1.149 (2)	C–O_{mean}[b]	1.138 (2)
Re–Mn(1)–Mn(2)	98.3 (1)	Re–H–Mn(1)	138.5 (3)
H–Re–C(1)	88.7 (1)	H–Re–C(2)	81.7 (2)
H–Re–C(3)	100.8 (2)	H–Re–C(4)	86.8 (1)
H–Re–C(5)	170.7 (2)	C(1)–Re–C(2)	88.9 (1)
C(1)–Re–C(3)	91.1 (1)	C(1)–Re–C(4)	175.4 (1)
C(1)–Re–C(5)	91.3 (1)	C(2)–Re–C(3)	177.4 (1)
C(2)–Re–C(4)	90.9 (1)	C(2)–Re–C(5)	88.9 (1)
C(3)–Re–C(4)	89.3 (1)	C(3)–Re–C(5)	88.5 (1)
C(4)–Re–C(5)	93.3 (1)	H–Mn(1)–C(6)	109.1 (2)
H–Mn(1)–C(7)	89.9 (2)	H–Mn(1)–C(8)	161.3 (3)
C(10)–Mn(2)–C(12)	90.1 (2)	C(10)–Mn(2)–C(13)	89.6 (2)
C(10)–Mn(2)–C(14)	168.7 (3)	C(11)–Mn(2)–C(12)	94.3 (2)
C(11)–Mn(2)–C(13)	94.8 (2)	C(11)–Mn(2)–C(14)	95.4 (2)
C(12)–Mn(2)–C(13)	170.8 (3)	C(12)–Mn(2)–C(14)	87.9 (2)
C(13)–Mn(2)–C(14)	90.6 (2)	Re–C(1)–O(1)	178.8 (2)
Re–C(2)–O(2)	177.8 (2)	Re–C(3)–O(3)	174.9 (2)
Re–C(4)–O(4)	177.9 (2)	Re–C(5)–O(5)	177.8 (2)
Mn(1)–C(6)–O(6)	174.4 (2)	Mn(1)–C(7)–O(7)	177.6 (2)
Mn(1)–C(8)–O(8)	177.6 (2)	Mn(1)–C(9)–O(9)	177.8 (2)
Mn(2)–C(10)–O(10)	179.4 (2)	Mn(2)–C(11)–O(11)	178.5 (2)
Mn(2)–C(12)–O(12)	177.2 (2)	Mn(2)–C(13)–O(13)	177.4 (2)
Mn(2)–C(14)–O(14)	178.5 (2)		

[a] Trans to Mn–Mn or Re–H–Mn. [b] Trans to M–CO.

There are no major differences between the geometry determined by X-ray diffraction at room temperature and the more precise low-temperature neutron diffraction results. The difference between equatorial and axial M–C distances[4] is still present with Re–C separations of 2.017 (7) Å (mean value) and 1.948 (2) Å for the equatorial and axial ligands, respectively; the corresponding mean values for the Mn–C distances being 1.862 (5) and 1.811 (3) Å (considering C(6), C(8), and C(11) to be axial). A small difference in mean C–O distances is also observed, viz., C–O mean 1.149 (2) Å (axial) vs 1.138 (2) Å (equatorial). It is noteworthy that the Re–Mn distance (3.316 (3) Å) determined at low temperature is significantly shorter than the room temperature X-ray value of 3.344 (1) Å, while the Mn–Mn values are equivalent within the standard deviation (2.909 (6) and 2.916 (1) Å). This may reflect the fact that the longer Re–H–Mn bond, being weaker, and therefore presumably possessing a more anharmonic stretching potential, is more affected by the temperature change.

A further observation supporting the relative weakness of the Re–Mn interaction is the large value of the Re–H–Mn angle (138.5 (3)°). When a strong M–M interaction (i.e., a short M–M separation) is present, this angle is ca. 110° (e.g., 103.3 (2)° in $[(PEt_3)_2(C_6Cl_5)Pt(\mu\text{-}H)Ag(H_2O)][CF_3SO_3]$ where the Pt–Ag distance is 2.750 (3) Å; these values are from a low-temperature neutron diffraction study[16]).

The hydride ligand is asymmetrically placed between the two metal atoms: Re–H 1.827 (4) Å and Mn–H 1.719 (5) Å. This difference is somewhat larger than the difference in covalent radii of Re and Mn (estimated to be 1.52 and 1.45 Å, respectively, from

---

(15) Brammer, L.; Howard, J. A. K.; Johnson, O.; Koetzle, T. F.; Spencer, J. L.; Stringer, A. M. *J. Chem. Soc., Chem. Commun.* **1991** 241–243.

(16) Albinati, A.; Chaloupka, S.; Demartin, F.; Koetzle, T. F.; Rüegger, H.; Venanzi, L. M.; Wolfer, M. K. Manuscript in preparation.

Table III. Metal-Metal Bond Distances (Å) for Some Mn and Re Complexes

compound	M–M	M–M′	M(H)M	ref
$Mn_2(CO)_{10}$	2.904 (1)			17
$Re_2(CO)_{10}$	3.041 (1)			17
$Mn(CO)_5Re(CO)_5$		2.909 (1)		28
$Re(CO)_4Cl(\mu\text{-}H)Re(CO)_4(NHMe_2)$			3.362 (1)	35
$Re(CO)_5(\mu\text{-}H)Re(CO)_4Re(CO)_5$	3.10 (1)		3.34 (1)	27
$Re(CO)_5(\mu\text{-}H)Re(CO)_4Mn(CO)_5$		2.960 (3)	3.392 (2)	26b
$Re(CO)_5(\mu\text{-}H)Mn(CO)_4Mn(CO)_5$	2.909 (6)		3.316 (3)	present work
$[Mn(CO)_5Mn(CO)_4Mn(CO)_5]^-$	2.906 (5) 2.883 (4)			36

the M–M separations in the isomorphous complexes $Re_2(CO)_{10}$ and $Mn_2(CO)_{10}$[17]).

The Mn–H distance in **1** is ca. 0.1 Å longer than that determined by neutron diffraction in $HMn(CO)_5$[18] (1.60 (2) Å). This difference is as expected[19] for a bridging vs terminal hydride, from observations reported for compounds having both bridging and terminal hydrides, e.g., $[(C_5Me_5)_2ThH(\mu\text{-}H)]_2$[20] and $[(PEt_3)_2Pt(\mu\text{-}H)_2Ir(H)_2(PEt_3)_2][BPh_4]$.[21] The Re–H bond distance in **1** (1.827 (4) Å) is shorter than the values of 1.878 (7) and 1.86 (4) Å found by neutron diffraction for the bridging hydrides in $[(PEt_2Ph)_2ReH_2(\mu\text{-}H)_2]_2$[22] and $[Et_4N][(triphos)Re(\mu\text{-}H)_3ReH_6]\cdot CH_3CN$,[23] respectively.

To our knowledge, there are to date only two other examples in which hydrides bridging two different metals have been precisely characterized by neutron diffraction: $[(PEt_3)_2Pt(\mu\text{-}H)_2IrH_2(PEt_3)_2][BPh_4]$[21] and $[(PEt_3)_2(C_6Cl_5)Pt(\mu\text{-}H)Ag(H_2O)][CF_3SO_3]$.[16] In both these compounds, a significant asymmetry in the bridge also is present (Pt–H = 1.731 (5) vs Ir–H = 1.881 (5) Å, and Pt–H = 1.674 (4) vs Ag–H = 1.831 (3) Å, respectively).

A particularly intriguing feature of the neutron diffraction results is the confirmation that **2** has cocrystallized with the major component, **1**. Cocrystallization of two structurally similar organometallic species in a single crystal has been previously observed[24,25] and is frequently utilized in EPR studies, where a single crystal containing a paramagnetic complex in a diamagnetic host is prepared.[24] For example, a single-crystal EPR study has been reported[24a,b] for the chromium radical $[(C_5H_5)Cr(CO)_3]$ doped into cystals of the diamagnetic compound $(C_5H_5)Mn(CO)_3$. Other examples include single-crystal EPR investigations of $[(C_5Me_5)Cr(CO)_3]$,[24c] $[(C_5Me_5)Cr(CO)_2(PMe_3)]$,[24c] $[Fe(CO)_3(PPh_3)_2]^+$,[24d] $[(C_5H_5)_2VS_5]$,[24e] and $[(CH_3C_5H_4)_2VCl_2]$.[24f] Yoon, Parkin, and Rheingold recently showed that apparent "bond-stretch isomers" of molybdenum oxo complexes actually result from cocrystallization of $MoOCl_2(PMe_2Ph)_3$ with small amounts of isostructural $MoCl_3(PMe_2Ph)_3$.[25] More pertinent to the Mn/Re species under consideration here are observations implying that partial occupancy of the Mn site by Re may also have been detected in the X-ray diffraction study of $(CO)_5Re(\mu\text{-}H)Re(CO)_4Mn(CO)_5$.[26] In their report of the structure determination of this compound, Churchill and Bau[26b] noted the very low displacement parameters for the Mn atom and suggested the possibility that a small amount of $(CO)_5Re(\mu\text{-}H)Re(CO)_4Re(CO)_5$ was present in their crystals. It is worth noting that while $(CO)_5Re(\mu\text{-}H)Re(CO)_4Mn(CO)_5$[26] is isomorphous and isostructural with the system reported herein (eclipsed conformation with respect to the hydride–bridged M–M bond), $(CO)_5Re(\mu\text{-}H)Re(CO)_4Re(CO)_5$[27] adopts a different conformation with the

Scheme I

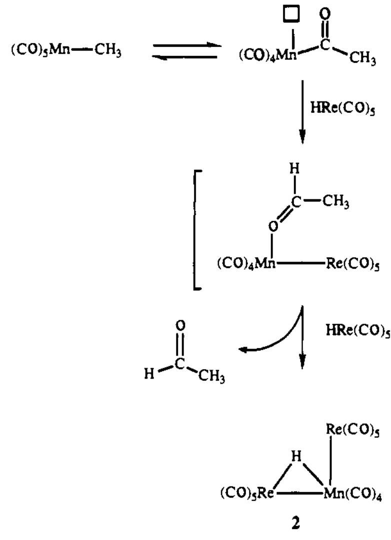

Scheme II

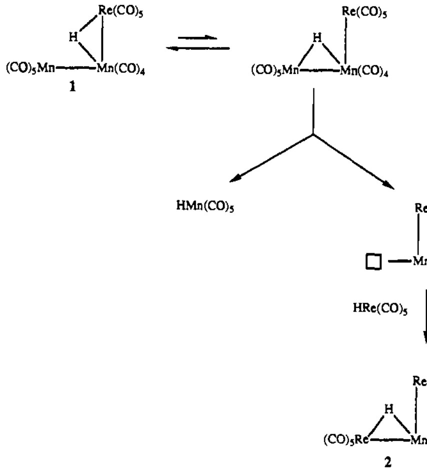

---

(17) Churchill, M. R.; Amoh, K. N.; Wasserman, H. J. *Inorg. Chem.* **1981**, *20*, 1609–1611.

(18) La Placa, S. J.; Hamilton, W. C.; Ibers, J. A.; Davison, A. *Inorg. Chem.* **1969**, *8*, 1928–1935.

(19) (a) Bau, R.; Teller, R. G.; Kirtley, S. W.; Koetzle, T. F. *Acc. Chem. Res.* **1979**, *12*, 176–183. (b) Peterson, J. L.; Dahl, L. F.; Williams, J. M. *Advances in Chemistry Series*; American Chemical Society: Washington, DC 1978; No. 167, pp 11–25.

(20) Broach, R. W.; Schultz, A. J.; Williams, J. M.; Brown, G. M.; Manriquez, J. M.; Fagan, P. J.; Marks, T. J. *Science* **1979**, *203*, 172–174.

(21) Albinati, A.; Emge, T. J.; Koetzle, T. F.; Meille, S. V.; Musco, A.; Venanzi, L. M. *Inorg. Chem.* **1986**, *25*, 4821–4827.

(22) Bau, R.; Carroll, W. E.; Teller, R. G.; Koetzle, T. F. *J. Am. Chem. Soc.* **1977**, *99*, 3872–3874.

(23) Abrahams, S. C.; Ginsberg, A. P.; Koetzle, T. F.; Marsh, P.; Sprinkle, C. R. *Inorg. Chem.* **1986**, *25*, 2500–2510.

(24) (a) Krusic, P. J.; McLain, S. J.; Morton, J. R.; Preston, K. F.; LePage, Y. *J. Magn. Reson.* **1987**, *74*, 72–81. (b) Morton, J. R.; Preston, K. F.; Cooley, N. A.; Baird, M. C.; Krusic, P. J.; McLain, S. J. *J. Chem. Soc., Faraday Trans. 1* **1987**, *83*, 3535–3540. (c) Fortier, S.; Baird, M. C.; Preston, K. F.; Morton, J. R.; Ziegler, T.; Jaeger, T. J.; Watkins, W. C.; MacNeil, J. H.; Watson, K. A.; Hensel, K.; Le Page, Y.; Charland, J.-P.; Williams, A. J. *J. Am. Chem. Soc.* **1991**, *113*, 542–551. (d) MacNeil, J. H.; Chiverton, A. C.; Fortier, S.; Baird, M. C.; Hynes, R. C.; Williams, A. J.; Preston, K. F.; Ziegler, T. *J. Am. Chem. Soc.* **1991**, *113*, 9834–9842. (e) Petersen, J. L.; Dahl, L. F. *J. Am. Chem. Soc.* **1975**, *97*, 6416–6422. (f) Petersen, J. L.; Dahl, L. F. *J. Am. Chem. Soc.* **1975**, *97*, 6422–6433.

(25) Yoon, K.; Parkin, G.; Rheingold, A. L. *J. Am. Chem. Soc.* **1991**, *131*, 1437–1438; **1992**, *114*, 2210–2218. For additional spectroscopic data on $MoOCl_2(PMe_2Ph)_3$ and $MoCl_3(PMe_2Ph)_3$, see: Desrochers, P. J.; Nebesny, K. W.; LaBarre, M. J.; Lincoln, S. E.; Loehr, T. M.; Enemark, J. H. *J. Am. Chem. Soc.* **1991**, *113*, 9193–9200.

(26) (a) Kaesz, H. D.; Bau, R.; Churchill, M. R. *J. Am. Chem. Soc.* **1967**, *89*, 2775–2776. (b) Churchill, M. R.; Bau, R. *Inorg. Chem.* **1967**, *6*, 2086–2092.

carbonyls at both terminal rhenium atoms staggered with respect to the central $Re(CO)_4$ unit and a Re–Re–Re angle of 107°. Thus we may assume that $(CO)_5Re(\mu\text{-}H)Re(CO)_4Re(CO)_5$ has two conformations of similar energy, with adoption of the one observed by Churchill and Bau[26] being forced by cocrystallization with $(CO)_5Re(\mu\text{-}H)Re(CO)_4Mn(CO)_5$. In any event, the replacement of a Mn–Mn bond by a Re–Mn bond, as has been found here, is not expected to produce large differences in the bond distances. See Table III for a comparison of metal–metal bond distances in the related compounds $Mn_2(CO)_{10}$,[17] $Re_2(CO)_{10}$,[17] and $(CO)_5MnRe(CO)_5$:[28] 2.904 (1), 3.041 (1), and 2.909 (1) Å.

Spectroscopic Characterization and Independent Synthesis of $(CO)_5Re(\mu\text{-}H)Mn(CO)_4Re(CO)_5$ (2). Along with a singlet at δ −19.66 in the ^1H NMR spectrum assigned to the bridging hydride of **1**, an additional singlet of lower intensity was observed at δ −19.24. The chemical shift of this resonance indicated it was also due to a bridging hydride. The spectroscopic data only indicated that the impurity was present in the bulk sample, but the single crystal neutron diffraction study discussed above demonstrated that the impurity had actually cocrystallized with the major product. Our assignment of this resonance to **2** is confirmed by independent synthesis of this complex from reaction of $CH_3Mn(CO)_5$ with $HRe(CO)_5$ in the manner reported previously by Warner and Norton.[6] The proposed mechanism for formation of **2** is shown in Scheme I. The formation of a coordinatively unsaturated acyl complex by migration of an alkyl group from a metal to a carbonyl has been clearly established in mechanistic studies of several related migration reactions.[29,30] The possible intermediacy of a complex containing an η^1-aldehyde ligand is supported by the isolation[30] of $Mn_2(CO)_9(\eta^1\text{-tolualdehyde})$ from the related reation of $(CO)_5Mn(p\text{-tolyl})$ with $HMn(CO)_5$. The fact that the η^1-aldehyde intermediate proposed in Scheme I was unobserved is not surprising in view of the facile displacement of the η^1-aldehyde ligand by $HRe(CO)_5$ in eq 1. Regardless of whether the mechanism actually involves an η^1-aldehyde intermediate or not, it is clear that this scheme accounts for the formation of **2**. It is important to note that this isomer of $HMnRe_2(CO)_{14}$ has Mn "in the middle" and is not the same as the complex of identical formula but different metal regiochemistry reported by Kaesz, Bau, and Churchill.[26] Their isomer of $HMnRe_2(CO)_{14}$ was $(CO)_5Re(\mu\text{-}H)Re(CO)_4Mn(CO)_5$, which has a terminal $Mn(CO)_5$.

Reactions with CO. The reaction of $(CO)_5Re(\mu\text{-}H)Re(CO)_4Mn(CO)_5$ with CO has been reported[26a] to produce $ReMn(CO)_{10}$ and $HRe(CO)_5$. We carried out analogous CO-induced cluster cleavage reactions, as shown in eqs 2 and 3. When a yellow-orange solution of **2** in C_6D_6 was treated with CO (1 atm), the color of the solution changed to pale yellow over ~30 min, and a quantitative yield of $HRe(CO)_5$ was observed by ^1H NMR. The bimetallic product was identified by IR as $ReMn(CO)_{10}$, with no contamination by $Mn_2(CO)_{10}$. In a similar experiment (eq 3), the reaction of **1** with CO also produced $HRe(CO)_5$. In this case, the predominant bimetallic product was $Mn_2(CO)_{10}$, but a small amount of $ReMn(CO)_{10}$ was also observed in the IR spectrum, consistent with the presence of the impurity **2** in the sample.

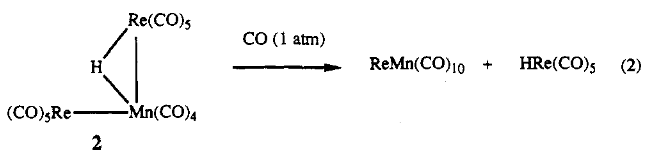

2

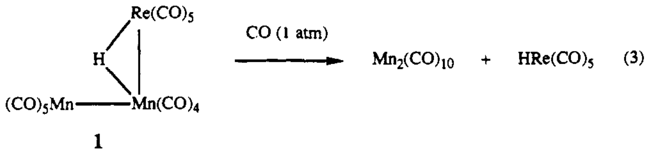

1

Mechanism for Metal–Metal Exchange. Having established **2** as the minor product that cocrystallized with **1**, we now consider the mechanism that accomplishes the conversion of a terminal $Mn(CO)_5$ moiety into $Re(CO)_5$. Fluxionality in metal clusters is frequently observed, and hydride mobility is particularly common.[31] The mechanism proposed in Scheme II accounts for the metal–metal exchange reaction that transforms **1** and $HRe(CO)_5$ into **2** and $HMn(CO)_5$. The initial equilibrium that converts the $Re(\mu\text{-}H)Mn$ complex into its $Mn(\mu\text{-}H)Mn$ isomer requires minimal movement of the hydride ligand. Hydride bridges between two metals are quite common,[3] but we are aware of few cases[32] of stable complexes that have a single hydride bridging two first-row metals with no additional bridging ligands. We suggest that the relative weakness of the $Mn(\mu\text{-}H)Mn$ bridge is a critical feature of this mechanism. Dissociation of $HMn(CO)_5$ from the proposed $(CO)_5Mn(\mu\text{-}H)Mn(CO)_4Re(CO)_5$ intermediate would give coordinatively unsaturated $ReMn(CO)_9$ (as in Scheme I, a square is used to represent a vacant coordination site), which would be rapidly trapped by $HRe(CO)_5$ to give the observed product **2**.

Determination of K_{eq} for the Mn/Re Exchange Equilibrium. When a C_6D_6 solution of **2** was treated with excess $HMn(CO)_5$, formation of $HRe(CO)_5$ and **1** was observed by ^1H NMR. The same Mn/Re exchange equilibrium (eq 4) was also approached from the other side by adding excess $HRe(CO)_5$ to a solution of **1**. The equilibrium constant for eq 4 was measured by adding an excess of both $HMn(CO)_5$ and $HRe(CO)_5$ to each cluster at 22 °C in C_6D_6 solution. The value obtained in this manner was $K_{eq} = 1.00 \pm 0.05$. This indicates that the Re–Mn bond is stronger than the Mn–Mn bond by about the same amount as the difference in bond dissociation enthalpy of $H\text{–}Re(CO)_5$ vs $H\text{–}Mn(CO)_5$. The reported bond dissociation energy[33] of $H\text{–}Re(CO)_5$ (75 kcal/mol) is 7 kcal/mol higher than that of $H\text{–}Mn(CO)_5$ (68 kcal/mol). Our results agree with mass spectroscopic measurements,[34] suggesting that the bond dissociation energy of the metal–metal bond of $MnRe(CO)_{10}$ exceeds that of $Mn_2(CO)_{10}$.

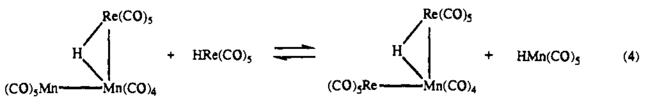

1 2

Acknowledgment. Research at Brookhaven National Laboratory and Argonne National Laboratory was carried out under Contracts DE-AC02-76CH00016 and W-31-109-ENG-38, respectively, with the U.S. Department of Energy, Office of Basic

---

(27) Yang, C. S.; Cheng, C. P.; Guo, L. W.; Wang, Y. *J. Chin. Chem. Soc.* (*Taipei*) **1985**, *32*, 17–22.

(28) Rheingold, A. L.; Meckstroth, W. K.; Ridge, D. P. *Inorg. Chem.* **1986**, *25*, 3706–3707.

(29) (a) Martin, B. D.; Warner, K. E.; Norton, J. R. *J. Am. Chem. Soc.* **1986**, *108*, 33–39. (b) Norton, J. R. *Acc. Chem. Res.* **1979**, *12*, 139–145. (c) Carter, W. J.; Okrasinski, S. J.; Norton, J. R. *Organometallics* **1985**, *4*, 1376–1386. (d) Nappa, M. J.; Santi, R.; Halpern, J. *Organometallics* **1985**, *4*, 34–41. (e) Jones, W. D.; Bergman, R. G. *J. Am. Chem. Soc.* **1979**, *101*, 5447–5449. (f) Jones, W. D.; Huggins, J. M.; Bergman, R. G. *J. Am. Chem. Soc.* **1981**, *103*, 4415–4423.

(30) (a) Bullock, R. M.; Rappoli, B. J.; Samsel, E. G.; Rheingold, A. L. *J. Chem. Soc., Chem. Commun.* **1989**, 261–263. (b) Bullock, R. M.; Rappoli, B. J. *J. Am. Chem. Soc.* **1991**, *113*, 1659–1669.

(31) For reviews treating various aspects of fluxionality of organometallic complexes, see: (a) Band, E.; Muetterties, E. L. *Chem. Rev.* **1978**, *78*, 639–658. (b) Evans, J. *Adv. Organomet. Chem.* **1977**, *16*, 319–347. (c) Mann, B. E. In *Comprehensive Organometallic Chemistry*; Wilkinson, G., Stone, F. G. A., Abel, E. W., Eds.; Pergamon: Oxford, 1982; Vol. 3, pp 89–171.

(32) Neutron diffraction study of $[Et_4N]^+[(CO)_5Cr(\mu\text{-}H)Cr(CO)_5]^-$: Roziere, J.; Wiliams, J. M.; Stewart, R. P., Jr.; Petersen, J. L.; Dahl, L. F. *J. Am. Chem. Soc.* **1977**, *99*, 4497–4499.

(33) Tilset, M.; Parker, V. D. *J. Am. Chem. Soc.* **1989**, *111*, 6711–6717; as modified in *J. Am. Chem. Soc.* **1990**, *112*, 2843.

(34) (a) Junk, G. A.; Svec, H. J. *J. Chem. Soc* (*A*) **1970**, 2102–2105. (b) Svec, H. J.; Junk, G. A. *J. Am. Chem. Soc.* **1967**, *89*, 2836–2840.

(35) Adams, R. D.; Kuhns, J. D. *Polyhedron* **1988**, *7*, 2543–2547.

(36) Bau, R.; Kirtley, S. W.; Sorrell, T. N.; Winarko, S. *J. Am. Chem. Soc.* **1974**, *96*, 988–993.

Energy Sciences. Support under NATO Grant 85/068 also is gratefully acknowledged. We thank Dr. Richard K. McMullan of Brookhaven National Laboratory for helpful discussions of the neutron structure refinement.

Supplementary Material Available: Table S1, atomic positional and anisotropic displacement parameters (1 page); Table S2, listing of observed and calculated squared structure factors (33 pages). Ordering information is given on any current masthead page.

Superexchange Metal–Metal Coupling in Dinuclear Pentaammineruthenium Complexes Incorporating a 1,4-Dicyanamidobenzene Dianion Bridging Ligand

M. A. S. Aquino,[†] **F. L. Lee,**[‡] **E. J. Gabe,**[‡] **C. Bensimon,**[‡] **J. E. Greedan,**[§] **and R. J. Crutchley***,[†]

Contribution from the Ottawa-Carleton Chemistry Institute, Carleton University, Ottawa, Canada K1S 5B6, the National Research Council of Canada, Chemistry Division, Ottawa, Canada K1A 0R6, and McMaster University, Institute for Materials Research, Hamilton, Ontario, Canada L8S 4M1. *Received September 25, 1991*

Abstract: Four dinuclear complexes, $\{\mu\text{-Dicyd-}[(NH_3)_5Ru]_2\}[ClO_4]_4$ (**1**), $\{\mu\text{-Me}_2\text{Dicyd-}[(NH_3)_5Ru]_2\}[ClO_4]_4$ (**2**), $\{\mu\text{-Cl}_2\text{Dicyd-}[(NH_3)_5Ru]_2\}[Cl]_4$ (**3**), and $\{\mu\text{-Cl}_4\text{Dicyd-}[(NH_3)_5Ru]_2\}[Cl]_4$ (**4**) where Dicyd^{2-} = 1,4-dicyanamidobenzene dianion, $\text{Me}_2\text{Dicyd}^{2-}$ = 1,4-dicyanamido-2,5-dimethylbenzene dianion, $\text{Cl}_2\text{Dicyd}^{2-}$ = 1,4-dicyanamido-2,5-dichlorobenzene dianion, and $\text{Cl}_4\text{Dicyd}^{2-}$ = 1,4-dicyanamido-2,3,5,6-tetrachlorobenzene dianion, have been synthesized. A crystal structure of the tosylate salt of **1** was determined. Two conformations of the dinuclear complex were revealed in the unit cell. For conformer **A**, both Ru(III)–cyanamide bonds are essentially linear, having a Ru(1)–N(6)–C(1) bond angle of 175°. For conformer **B**, both Ru(III)–cyanamide bonds are bent, having a corresponding bond angle of 150°. In both conformers, the Dicyd^{2-} bridging ligand is planar with the cyanamide groups in an anti configuration. Crystal structure data for the complex are space group $P2_1/a$, with a, b, and c = 7.5861 (6), 23.0450 (19), and 32.078 (3) Å, respectively, β = 95.771 (7)°, V = 5579.5 Å^3, and Z = 4. The structure was refined using 3947 significant Cu (1.54056 Å) reflections to an R factor of 0.063. The dinuclear complexes were characterized by cyclic voltammetry, UV–vis NIR spectroscopy, and magnetic susceptibility. The mixed-valence complexes [Ru(III), Ru(II)] of **1**–**4** were shown to be weak coupling cases with the order of coupling inferred from comproportionation constants at **1** < **4** < **3** < **2**. Temperature dependent magnetic susceptibility measurements of the oxidized complexes [Ru(III), Ru(III)] of **1**–**4** showed antiferromagnetic behavior. Isotropic spin only models of the data for **3** and **4** and the tosylate salt of **1** derived magnetic exchange coupling constants of J = −95.9, −61.9, and −100 cm^{-1}, respectively (where $\mathcal{H} = -2J\hat{S}_a{\cdot}\hat{S}_b$). For the perchlorate salt of **1**, a slight rise in magnetic susceptibility as temperature approached 300 K allowed an estimate of $J \geq -400$ cm^{-1}. For **2**, antiferromagnetic coupling was of sufficient magnitude to render the complex diamagnetic at room temperature. Antiferromagnetic coupling of this magnitude at an estimated through space separation of 13.2 Å is unprecedented. Coupling in both mixed-valence and oxidized complexes is suggested to be dominated by a superexchange mechanism involving the Ru(III) dπ-orbitals and the π HOMO of the Dicyd^{2-} bridging ligand. Extended Huckel calculations have been performed using the crystal structure data of the free Dicyd^{2-} ligands to illustrate that a continuous π interaction between metal ions is possible.

Introduction

The purposeful synthesis of novel magnetic or electronic solid state materials requires a fundamental grasp of the underlying *molecular* properties of the unit building blocks that make up the crystal lattice. The goal is to be able to design the properties of a molecular unit and to assemble these units in a manner which expresses the desired *macroscopic* property. This idea is not new, but the design of molecular units that express potentially useful molecular properties is a field with considerable potential for development requiring contributions from all fields of chemistry and has additional application to the construction of molecular electronic devices.[1]

One strategy for the construction of a magnetic material has been to assemble molecular units composed of heterodinuclear complexes with total spin $S > 0$ in which the metal ions are antiferromagnetically coupled.[2] Room temperature magnetism requires that coupling between metal ions within molecular units and between molecular units be of sufficient magnitude to prevent randomization of spin. It is therefore essential that the means by which metal–metal coupling can be propagated be fully explored to provide the optimum parameters for molecular unit design and synthesis.

The weak coupling of two metal ions bridged by a ligand has been long ascribed to a superexchange mechanism[3,4] in which metal ion states are mixed by virtual electronic states of the bridging ligand. These virtual states can be conceptualized as ones in which the bridging ligand can be either reduced (electron-type) or oxidized (hole-type). Consistent with the weak coupling of metal ions and the treatment of these systems by perturbation theory,[4,5] neither electron nor hole should be thought of as vibronically localized on the bridge. The bridge molecular

---

[†] Ottawa-Carleton Chemistry Institute, Carleton University.

[‡] National Research Council of Canada.

[§] McMaster University, Institute for Materials Research.

(1) (a) *Molecular Electronic Devices II*; Carter, F. L., Ed.; Marcel Dekker: New York, 1987. (b) *Molecular Electronics: Science and Technology*; Aviram, A., Ed.; Engineering Foundation: New York, 1989. (c) Beratan, D. N. *Mol. Cryst. Liq. Cryst.* **199**, *190*, 85.

(2) For example, see: Kahn, O.; Pei, Y.; Verdaguer, M.; Renard, J. P.; Sletten, J. *J. Am. Chem. Soc.* **1988**, *110*, 782. Pei, Y.; Kahn, O.; Nakatani, K.; Codjovi, E.; Mathoniere, C.; Sletten, J. *J. Am. Chem. Soc.* **1991**, *113*, 6558 and references therein.

(3) Kramers, H. A. *Physica* **1934**, *1*, 182.

(4) McConnell, H. M. *J. Chem. Phys.* **1961**, *35*, 508.

(5) Kosloff, R.; Ratner, M. A. *Isr. J. Chem.* **1990**, *30*, 45.

0002-7863/92/1514-5130$03.00/0